Journal of Inorganic Biochemistry 194 (2019) 214–222

Contents lists available at ScienceDirect

Journal of Inorganic Biochemistry

journal homepage: www.elsevier.com/locate/jinorgbio

What is pure hemozoin? A close look at the surface of the malaria pigment

E. Danae Guerra[a], Fadi Baakdah[b], Elias Georges[b], D. Scott Bohle[c], Marta Cerruti[a,*]

[a] Department of Mining and Materials Engineering, McGill University, Montreal, Quebec H3A 2B2, Canada
[b] Institute of Parasitology, McGill University, Ste Anne de Bellevue, Quebec H9X 3V9, Canada
[c] Department of Chemistry, McGill University, Montreal, Quebec H3A 0B8, Canada

ARTICLE INFO

Keywords:
Hemozoin
Malaria pigment
Surface
Purification
Contamination
Characterization

ABSTRACT

The malaria parasite, *Plasmodium* spp., produces hemozoin (Hz) crystals as a by-product of hemoglobin digestion. Purification methods used to remove host or parasite products adsorbed on Hz surface lead to variable and undetermined residues. This compositional variation likely accounts for the assortment of contradictory results in studies of Hz's biomineralization, immunomodulating properties, and the mechanism of action of some antimalarials. In this work, we study the surface of Hz cleaned with two methods, both reported in the literature, one stricter than the other. We find that biomolecules are adsorbed on Hz treated with either method, they bind through carboxylate groups, and may be present within Hz structure. Their composition and amount depend on the washing protocol, which also introduces contaminants. This finding led us to question the concept of "pure" Hz, and to propose x-ray photoelectron spectroscopy (XPS) and matrix-assisted laser desorption/ionization time of flight (MALDI-TOF) as characterization tools to assess surface contamination prior to further work on Hz crystals.

1. Introduction

Malaria is a blood infection caused by parasites of the *Plasmodium* genus, causing an estimated 216 million infections annually and almost half million deaths worldwide [1]. During the intraerythrocytic asexual stage of *Plasmodium*, the parasite feeds from hemoglobin to sustain its development [2], with the released heme rapidly converted into an insoluble crystal called hemozoin (Hz) as a detoxification mechanism [2]. Hz, also known as "malaria pigment" due to its dark brown color, is a crystalline biomineral, consisting of dimers of heme linked reciprocally by iron-carboxylate bonds; the dimers are further arranged in chains linked by hydrogen bonds [3]. Lipids, proteins, the digestive vacuole membrane and acidic pH are thought to play significant roles in Hz biomineralization; however, the overall process is still not entirely resolved [2].

Hz formation is the target of several quinoline-derived antimalarials, and possibly artemisinins, which are thought to inhibit Hz growth either by forming drug-heme complexes or by adsorbing on Hz surface [4]. Given the widespread parasitic resistance to these antimalarials, a deeper understanding of their mechanism of action and of the mechanism of Hz biomineralization [5] are topics of utmost urgency.

Hz seems to be also involved in the immunopathology of malaria. Many studies have investigated this by adding Hz or its synthetic counterpart, hematin anhydride (HA) to phagocytic cell cultures [2], but the results are often contradictory and poorly reproducible [6]. For example, several groups reported that Hz and HA induce the production of pro-inflammatory cytokines and chemokines [7–9], while others have reported that HA decreases the anti-inflammatory response [10]. Hz also contributes to malarial anemia by suppressing red blood cells (RBC) proliferation [11–13]; but HA has lower activity compared to Hz [11].

Both using HA and Hz to perform these experiments has challenges: different preparations of HA result in crystals with varied morphology and size, which impact their surface reactivity [14]; and when Hz is isolated from schizonts, various biomolecules bind to Hz surface [2]. Such components may be lipids, parasitic DNA, fibrinogen, digestive vacuole membrane residues, RBC membranes [2] and fibrin during placental infection [15]. These compounds could be involved in the biological effects observed in Hz; thus, it is still not clear whether the immune activity of Hz is caused by the crystals themselves or by its surface contaminants [2].

The lack of a standardized protocol to purify native Hz after its extraction contributes to the difficulties in studying Hz formation and properties [2,16]. The methodologies reported aim to remove a variety of biomolecules that are thought to adhere to Hz during parasite

* Corresponding author at: 3610 University Street, 2M020 Wong Building, Montreal, QC H3A 0C5, Canada.
E-mail address: marta.cerruti@mcgill.ca (M. Cerruti).

https://doi.org/10.1016/j.jinorgbio.2019.01.021
Received 28 November 2018; Received in revised form 14 January 2019; Accepted 17 January 2019
Available online 16 February 2019
0162-0134/

incubation and lysis [6]. The procedures to purify Hz include washing the crude extract with a hypotonic solution of phosphate buffer saline (PBS) [17]; separation of Hz from cell debris by ultrafiltration and/or magnetic-activated cell sorting (MACS) separators [18]. Other procedures involve extracting the proteins with organic solvents and water [19], or digesting Hz organic coating by proteinase K, followed by washes with a detergent and urea [20]. More thorough treatments include a combination of organic solvents, extensive digestion by proteinase K, DNase I and RNase A, and final washes with detergents and water [21]. Clearly, the different methods used to purify Hz may produce crystals with different compositions, which would ultimately impact the host response and produce the observed contradictory results [9]. Hence, to clarify these issues, the surface of Hz should be carefully studied after its extraction and purification [6].

Surprisingly, not many studies focus on Hz surface. The few studies on this topic analyze crystal morphology and size [3,22,23], or are carried out on HA [4,14]. The elemental composition, atomic environment and main adsorption sites of Hz surface are still unknown. Moreover, none study how the purification method influences Hz surface.

In this report, we address this knowledge gap by analyzing the surface of Hz with XPS to study the composition and chemical environment of atoms on Hz surface, and MALDI-ToF to understand the nature of the adsorbed molecules. We washed Hz with an extensive purification procedure in an attempt to obtain highly pure crystals; this methodology includes using organic solvents and water to precipitate proteins [19], three types of enzymes, detergents and water [21]. We also performed a shortened version of the same protocol to study the impact of the cleaning procedure on the surface composition. Then, we compared these samples to HA, since these crystals are devoid of adsorbed organic matter [2], and suspended HA in solutions that mimic the natural environment of Hz to assess the sources of the organic components adsorbed on Hz and its surface adsorption sites.

2. Experimental

2.1. Materials

Reagent grade sinapinic acid (SA), trifluoroacetic acid (TFA), acetonitrile and calcium chloride were obtained from Sigma-Aldrich Canada. Methanol, chloroform, sodium chloride, magnesium chloride hexahydrate and sodium hydroxide pellets ACS grade were purchased from Fisher Scientific. Proteinase K (20 mg/mL) PCR grade, DNase I (100 U/mL), RNase A (DNase and protease-free, 10 mg/mL) and Halt protease inhibitor (single use cocktail, 100×) were obtained from Thermofisher Scientific. *N*-2-hydroxyethylpiperazine-*N′*-2-ethanosulfonic acid (HEPES), L-glutamine and RPMI1640 were purchased from Gibco (by Life Technologies), saponin from *Quillaja saponaria* Molina, practical grade from Acros Organics MS and sorbitol from Sigma life sciences. A+ blood was obtained from The Interstate Blood Bank, INC.

Stock solutions of 25 mM HEPES, 0.05% saponin in PBS (1×) were prepared in advance. Also, 2% sodium dodecyl sulfate (SDS), phosphate-buffer saline solution (PBS 1×, pH 7.4), 10 mM Tris hydrochloride (Tris-HCl, pH 8) and 10 mM 3-[(3-Cholamidopropyl)dimethylammonio]-1-propanesulfonate hydrate (CHAPS) were prepared from reagents purchased from BioShop, Canada Inc. The 10 mM CHAPS buffer was prepared by mixing 150 mM NaCl, 1 mM $CaCl_2$ and the protease inhibitor in 50 mM Tris HCl, the pH was adjusted to 7.4.

Proteinase K (2 mg/mL) was prepared in a buffer solution of 2% SDS/Tris-HCl, pH 8. DNase I (100 U/mL) and RNase A (1 mg/mL) were mixed in the same buffer solution consisting of 10 mM Tris-HCl, 2.5 mM $MgCl_2$ and 0.5 mM $CaCl_2$, pH 8.0. The pH of the stock solutions was adjusted with 0.1 M HCl or 0.1 M NaOH (reagents were ACS plus grade, purchased from Fisher Scientific). Milli-Q water from a Barnstead purification system (resistivity of 18.2 MΩ-cm) was used to prepare all the solutions and experiments unless specified. Protein LoBind tubes were purchased from Eppendorf.

2.2. Methods

2.2.1. Cultivation of P. falciparum asexual blood stages and Hz extraction

Plasmodium falciparum chloroquine sensitive strain 3D7-H was maintained in a synchronous culture by implementing a modified version of Trager and Jensen's cultivation method [24]. In brief, parasites were cultivated in RPMI 1640 media supplemented with L-Glutamine and 25 mM HEPES in 10% human plasma and A+ human erythrocytes in a 2% hematocrit. 5% sorbitol was used for synchronization of the parasite blood stages. The parasites were collected at the late trophozoite stage and processed as follows: washed in PBS, treated with 0.05% saponin in PBS to lyse the RBC, washed in PBS and extracted in CHAPS buffer, and finally centrifuged at 15 k rpm for 10 min at 4 °C. The supernatant was removed to give cytosolic free samples of Hz, followed by re-suspension in PBS to store at 4 °C for further cleansing steps.

2.2.2. Extensive washing of hemozoin (ewHz)

This method of purification followed what Lvova *et al.* reported, with minor modifications [21]. Each sample consisted of 300 μL of Hz suspended in the lysis buffer. The sample was centrifuged for 1 min at 9000 rpm and the supernatant removed. Protein traces were removed by extraction with chloroform, methanol and water, according to the Wessel and Flügge method [19]. Briefly, 400 μL of methanol were added and the sample was vortexed until obtaining a uniform suspension, followed by centrifugation (30 s at 9000 rpm). Then, 200 μL of chloroform were added and the sample was vortexed and centrifuged again (30 s at 9000 rpm). 300 μL of water were added and the suspension was vortexed and centrifuged (2 min, 9000 rpm). The top phase was removed, 300 μL of methanol were added and the pellet was mixed and centrifuged (2 min, 9000 rpm). The supernatant was removed, and the resulting Hz was treated with 2 mL proteinase K (2 mg/mL); the suspension was gently mixed by flipping the tube upside down, and was left at 37 °C for 18 h. After this time, the suspension was centrifuged at 14,000 rpm for 20 min, the supernatant discarded and the pellet washed three times (2% SDS, 10 mM Tris-HCl, pH 8) with centrifugation in between and supernatant discarded. Later, the resulting material was treated with 2 mL of a solution of DNase I (100 U/mL) and RNase A (1 mg/mL) for 2 h at 37 °C. The suspension was centrifuged at 14,000 rpm for 20 min and the top phase removed. Then, the crystals were washed three times with a solution of 2% SDS and three times with milli-Q water. The resulting sample was dried at room temperature and stored under vacuum prior to the characterization. This sample is referred to as ewHz in the text.

2.2.3. Partial washing of Hz (pwHz)

As described in Section 2, Hz was first purified using the Wessel-Flügge method [19] to precipitate most of the proteins and lipids, followed by a treatment with 2 mL of a solution of proteinase K (2 mg/mL) for 18 h at 37 °C. The resulting material was washed three times with a solution of 2% SDS/Tris-HCl (pH 8), and three times with milli-Q water with centrifugation in between steps and supernatant removal. The sample was dried at room temperature and kept under vacuum until characterization. This sample is referred to as pwHz in the text, since it involves only one enzyme (proteinase K) to digest the surface contaminants of Hz, and lacks DNase I and RNase A.

2.2.4. Characterization techniques

The surface composition of all materials was studied by X-ray photoelectron spectroscopy (XPS) using a spectrometer from Thermo Scientific K*α*, equipped with an Al cathode with an incident K*α* radiation of 1486 eV, and a spot diameter of 200 μm. A flood gun of low energy electrons was used to prevent surface charging during the measurement. The analyses were carried out with a pass energy of 1 eV for all survey scans, and 0.1 eV for high resolution scans of individual

core levels. Data processing was performed using Avantage Software version 5.956, using Gaussian-Voigt curve functions, while the background was removed using the Smart method. Peaks in the elemental high resolution spectra were fitted according to the parameters reported in Supporting information Tables S1 and S2. Three points were randomly selected along each sample and at least three samples were analyzed. High-resolution spectral energies were normalized by fixing the position of the C-C/C=C component of C_{1s} at 284.5 eV.

Matrix-assisted laser desorption/ionization time of flight (MALDI-ToF) was used to compare the adsorbed biomolecules of Hz to the surface of HA. To prepare the matrix, 20 mg/mL of sinapinic acid (SA) were dissolved in a mixture of 70:30 v/v acetonitrile:trifluoroacetic acid (0.1%, prepared in water). The mixture was vortexed, followed by centrifugation at 5000 rpm for 1 min to remove the excess of SA. The supernatant was transferred to another tube to be used as matrix, while undissolved SA was discarded. The sample (Hz or HA) was mixed thoroughly with 10 µL of matrix; then, 3 µL of this suspension were dropped on the stainless steel MALDI target plate and dried under a stream of air. The analysis was performed on an Autoflex II smartbeam MALDI-ToF mass spectrometer (Bruker Daltonik GmBH), equipped with a frequency-tripled Nd:YAG laser of 355 nm and frequency of 200 Hz. Measurements were performed in the positive ion reflectron mode with an accelerating voltage of 20 kV, with detector bias gating set to 1.3 kV. The power was set at 20% with a global attenuator offset at 80%, reflectron at 10× and the digitizer was fixed at 1.0. Three spots were selected along each sample and at least three samples were analyzed. The spectra were produced by averaging 30 consecutive shots. The data was normalized with respect to the intensity of the peak at 616 Da, which corresponds to the molecular mass of heme.

2.2.5. Statistical analysis

Three independent experiments were performed for each sample. All the data are expressed as mean ± standard deviation (SD). Means that are statistically different are indicated with a subscript asterisk (*). Microsoft Excel 2016 was used to perform the One-way ANOVA tests followed by Bonferroni's test correction to evaluate the statistical difference of multiple samples, where $P < 0.01$ was considered a significant difference.

3. Results

3.1. The cleaning method impacts the composition and amount of residual biomolecules on Hz surface

A flow chart for the purification of Hz is shown in Fig. 1A with the main distinction between extensively washed Hz (ewHz) and partially washed Hz (pwHz) being the steps after proteinase K treatment. Survey XPS analysis for ewHz shows the expected elements of C, O, N and Fe (Fig. 1B, red), and the atomic percentages of this sample do not show significant differences compared to HA (Fig. 1B, gray). No other elements were found on this sample. The lack of magnesium, phosphorus, and zinc on both, ewHz (Fig. 1B, red) and on pwHz (Fig. 1B, blue) clearly indicates that nucleic acids, with their phosphate backbone and zinc and magnesium counterions [25], are not present. The absence of sulfur and sodium in all the samples also indicates that sodium dodecyl sulfate was removed after the rinses with water, or at least its concentration was below XPS detection limit of 1 to 0.1 atomic % [26].

In contrast, the sample treated with fewer enzymes, pwHz, shows the unexpected presence of Si and Ca (Fig. 1B, blue). To determine if these elements are contaminants resulting from the purification, we studied the surface composition of dead *Plasmodium* parasites of the same strain and clone cultivated to obtain Hz (*Plasmodium falciparum* 3D7). We rinsed the dead parasites with hexane and dichloromethane to extract the water and facilitate drying (see Supporting information Section S2 for details) for XPS analysis. We found Si in this sample (Fig. S1), which suggests that this element is *Plasmodium*-derived. The origin of Si in *Plasmodium* is unclear, as to date there is no information about this element in apicomplexan parasites. Nevertheless, there is evidence indicating an important role of silicon in bone and connective tissue health [27], and in plant defense [28].

We did not detect significant concentration of calcium in the elemental composition of the parasites; however, Ca is critical for vital functions in apicomplexan parasites, such as host cell invasion and egress, motility and differentiation [29,30]. In *Plasmodium*, this element could originate from its intracellular constituents, such as the endoplasmic reticulum, acidocalcisomes, mitochondria, Golgi apparatus, nuclei, or the food vacuole where Hz is produced [29,31]. Since XPS is a highly surface-sensitive technique, we may not have sampled these inner storage organelles, which explains why we did not find Ca in the dead parasites.

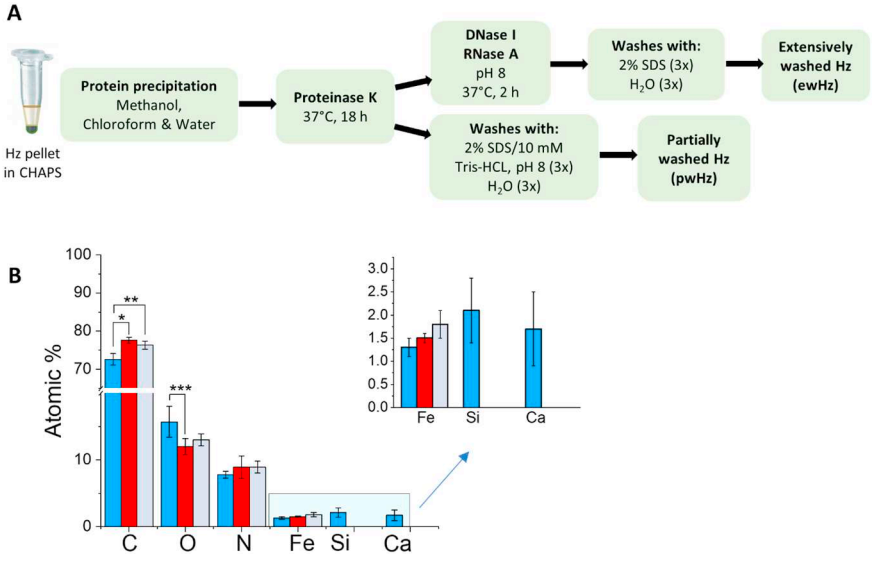

Fig. 1. (A) Flow chart of the methodologies used to treat Hz to produce pwHz and ewHz. (B) Elemental composition of pwHz (*blue bars*) and ewHz (*red bars*) evaluated by XPS and compared with HA (*gray bars*). Values represent mean ± SD calculated for three independent experiments and three different spots analyzed along the same sample. *Significant differences between area ratios, with $*P < 0.0004$, $**P < 0.003$ and $***P < 0.002$. (For interpretation of the references to color in this figure legend, the reader is referred to the web version of this article.)

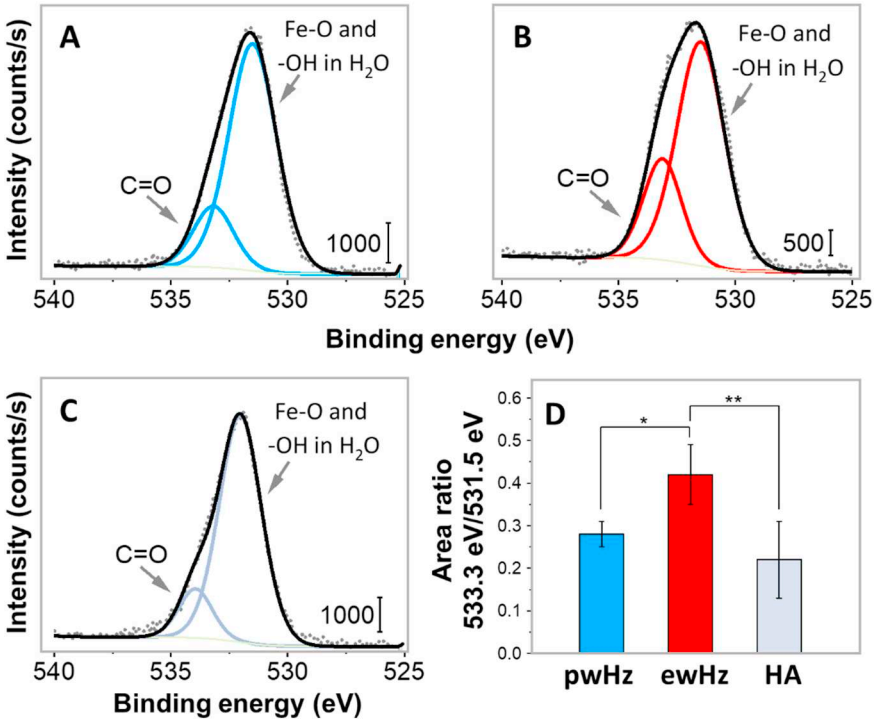

Fig. 2. XPS high-resolution spectra of the O_{1s} level collected for (A) pwHz (B) ewHz, and (C) HA. Experimental data are shown in dark gray dotted line, peak fits in continuous blue, red or light gray (A, B, or C, respectively), and the overall fit in black. (D) Area ratios of the 533.3 eV/531.5 eV peaks for the O_{1s} core level measured for pwHz (*blue bar*), ewHz (*red bar*), and HA (*gray bar*). Values represent mean ± SD calculated for three independent samples and three different spots analyzed along the same sample. *Significant differences between area ratios, with $*P < 0.0003$ and $**P < 0.006$. (For interpretation of the references to color in this figure legend, the reader is referred to the web version of this article.)

The atomic percentages of N and Fe in pwHZ are close to the theoretical values, while C is significantly lower and O significantly larger (Fig. 1B, blue). To understand these differences as well as learn more about the nature of the adsorbed biomolecules on Hz, we ran high resolution XPS measurements for O, N, C and Fe on both pwHz and ewHz, and compared them to those measured on pure HA. C_{1s} and Fe_{2p} spectra do not show significant differences between the two samples (Fig. S2).

High resolution O_{1s} spectra of pwHz, ewHz and HA (Fig. 2A–C) show a peak located at 531.5 eV that corresponds to both the Fe-O-C(O) bond and the –OH group of water adsorbed on the crystals surface; while the peak at 533.5 eV is assigned to C═O from carboxylates of the propionic side chains [14]. In the absence of water, the 531.5 and the 533.4 eV peaks should have the same areas since there are four oxygen atoms of each type in the crystalline structure of both Hz and HA [14]. However, HA and Hz are hygroscopic, with the crystals being able to absorb up to 14% of its mass in water on their surface and possibly within the heme layers [32].

In pwHz, the 533.3 eV/531.5 eV peak area ratio is close to HA (Fig. 2D); this suggests that water may be associated with the adsorbed species on pwHz. These compounds may be constituted by small peptides, which were not digested by proteinase K alone, and are prone to interact with water [33]. This is in good agreement with the high oxygen content in this sample, as discussed earlier (Fig. 1B, blue bars). Conversely, in ewHz the 533.3 eV/531.5 eV peak area ratio is significantly larger than in pwHz and HA (Fig. 2D). This indicates less water on the surface of ewHz, probably due to fewer adsorbed species on it, resulting in a surface with more –COOH groups exposed. Although ewHz is very close to HA in composition, the difference in water content most likely arises due to the methodology used to synthesize the HA used in this work (**Supporting Information Section S1**). While the XPS high resolution spectra of C_{1s}, N_{1s} and Fe_{2p} from HA among methods are equivalent, the O_{1s} spectra show varied water content among synthesis methods, as demonstrated in a previous work [14]. Therefore, it can be expected that ewHz and HA differ in amount of water adsorbed.

The analysis of the N_{1s} spectra of pwHz and ewHz (Fig. 3A and B, respectively) show an intense peak at 398.2 eV, which corresponds to the four equivalent N—Fe bonds in the pyrrole of each porphyrin ring, as confirmed by their presence also in the spectrum of HA (Fig. 3C) [14]. Both samples also show a peak at around 401 eV that is related to the π-π* transition of the delocalized electrons, as shown for HA [14]. However, the 401 eV/398.2 eV peak area ratio in pwHz (Fig. 3D, blue) is significantly higher than that in ewHz (Fig. 3D, red) and HA (Fig. 3D, gray). This could be related to a contribution from sp^2 hybridized nitrogen components (sp^2-N) derived from the adsorbed biomolecules [34]. Both pwHz and ewHz show a new signal at 399.2 and 399.7 eV, respectively, which may arise from sp^3 hybridized nitrogen components (sp^3-N) bound or adsorbed onto the surface of the crystals. Overall, the significantly higher area ratios (both 401 eV/398 eV and 399.2 eV/398.2 eV) in pwHz (Fig. 3D, blue) confirm that larger quantities of biomolecules are adsorbed on the surface of these crystals.

3.2. Residual biomolecules adsorbed on Hz surface are related to protein fragments or amino acids

To assess the origin of the adsorbed biomolecules found on pwHz and ewHz, we put our synthetic model crystal, HA, in contact with compounds that are part of the natural cycle of Hz production or extraction, i.e. parasite schizont lysates and RBC membranes, respectively. HA crystals were incubated with these components at 37 °C for 24 h, and then treated with the same extensive purification procedure used to obtain ewHz (Supporting information Sections S5.1 and S5.2). Additionally, we prepared a control sample of HA only treated with the extensive purification used to produce ewHz (see Experimental Section 2.2.2), to investigate whether the methods and enzymes used can introduce additional adsorbed molecules on Hz. We studied these materials with XPS and analyzed the high resolution N_{1s} spectra to compare with what was found on ewHz and pwHz.

First, we put HA crystals in contact with dead parasite lysates. The XPS N_{1s} spectra (Fig. 4A) show three peaks centered at 398.1, 399.7 and 401.2 eV. The location of these peaks is very close to the signals found on pwHz and ewHz (Fig. 3A and B, respectively), indicating a possible contribution of parasite cell debris, constituted mostly by aggregated and denatured plasmodial proteins [35] on the surface of these samples. However, the 399.7 eV/398.2 eV peak area ratio in this sample (Fig. 4D, turquoise) is lower compared to that found on pwHz and ewHz

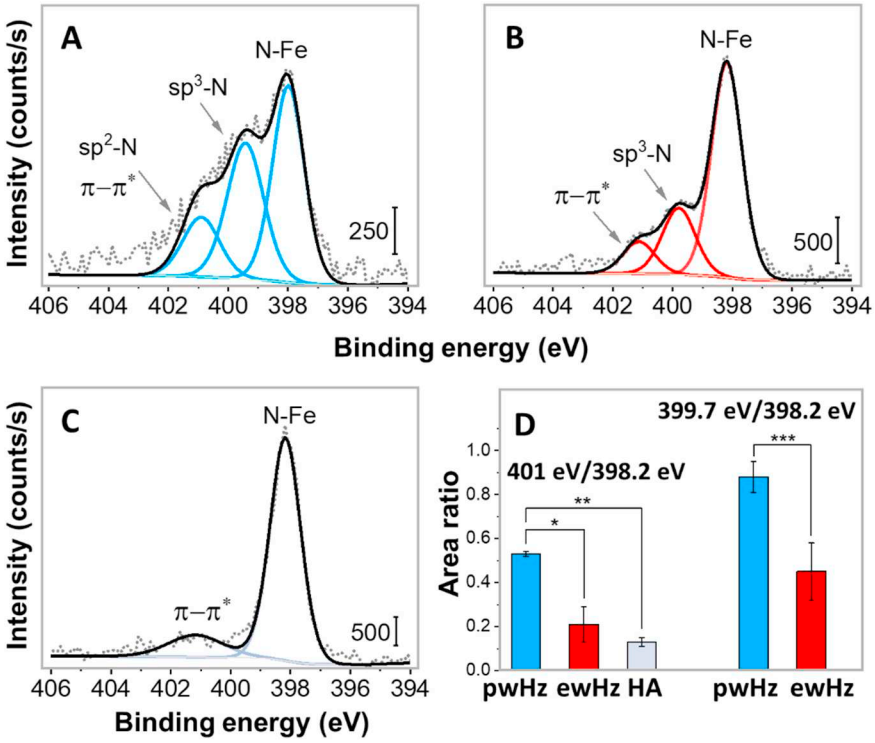

Fig. 3. XPS high-resolution spectra of the N_{1s} core level collected for (A) pwHz (B) ewHz and (C) HA. The dashed blue line in pwHz distinguishes the contribution from the π-π* delocalization. Experimental data are shown in dark gray dotted line, peak fits in blue, red or light gray, and the overall fit in black. (D) Area ratios of the XPS N_{1s} 401.0 eV/398.2 eV and 399.7 eV/398.2 eV peaks acquired for pwHz (*blue bars*), ewHz (*red bars*), and HA (*gray bars*). Values represent mean ± SD calculated for three independent experiments and three different spots analyzed along the same sample. *Significant differences between area ratios, with $*P < 9 \times 10^{-7}$, $**P < 5 \times 10^{-8}$ and $***P < 1 \times 10^{-6}$. (For interpretation of the references to color in this figure legend, the reader is referred to the web version of this article.)

(Fig. 3D). This indicates that part of the residual sp^3-N components in pwHz and ewHz arise from other biological sources, besides schizont debris.

Then, we tested the interaction of HA with RBC membranes. The XPS analysis revealed three peaks in the N_{1s} spectra of this sample (Fig. 4B) at 398.1, 399.8 and 401.1 eV, again very close to the peak locations measured on pwHz and ewHz (Fig. 3A and B, respectively), indicating that residues of RBC membranes interact strongly with Hz and may be predominant on the surface of the crystals [35]. Indeed, the high 399.7 eV/398.2 eV area ratio in this control (Fig. 4D, yellow) suggests that many of the sp^3-N species adsorbed on pwHz and ewHz derive from the interaction between RBC membranes and HA, despite the extensive washes. These results suggest a strong affinity between Hz and hemoglobin components that may attach during the process of Hz formation, as proposed by Goldie *et al.* [35], or during Hz release [36,37].

Finally, we looked at the N_{1s} spectrum of HA treated with the thorough purification used to produce ewHz, to understand if the purification itself may introduce adsorbed biomolecules on Hz. The XPS N_{1s} spectrum (Fig. 4C) presents three peaks located at 398.1, 399.7 and 401.3 eV. The similarity between this spectrum and those recorded for ewHz and pwHz (Fig. 3A and B) shows that the adsorbed biomolecules

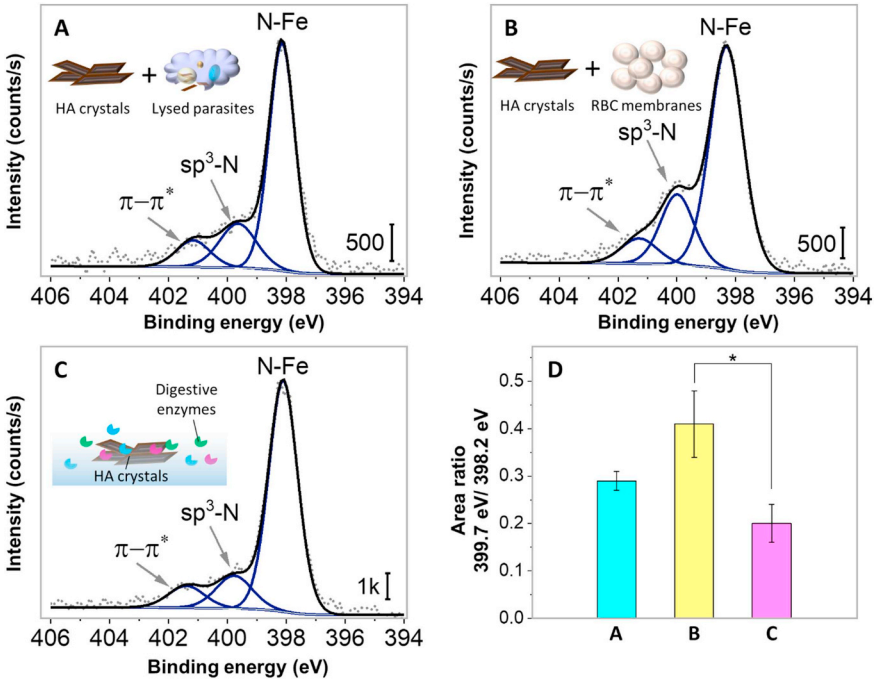

Fig. 4. XPS high resolution of the N_{1s} core level acquired for purified HA after suspension in (A) dead parasites of *P. falciparum* of the clone 3D7, (B) RBC membranes, (C) enzymes and detergents used to prepare ewHz. Experimental data are shown in dark gray dotted line, peak fits in blue and the overall fit in black. (D) N_{1s} 399.7 eV/398.2 eV peak area ratio calculated for the spectra shown in A, B and C. *Significant differences between area ratios, with $*P < 0.006$. Values represent mean ± SD calculated for three independent experiments and three different spots analyzed along the same sample. (For interpretation of the references to color in this figure legend, the reader is referred to the web version of this article.)

found on the surface of pwHz and ewHz could also arise from the purification process itself. These compounds could be either fragments of proteins degraded by the enzymes used during the purification, or fragments of the enzymes themselves. However, the 399.7 eV/398.2 eV peak area ratio (Fig. 4D, pink) is significantly smaller compared to pwHz and ewHz (Fig. 3D, blue and red, respectively), indicating that even though the purification step may be introducing contamination on Hz, it is not the only source of organic material containing sp^3-N compounds on Hz surface.

Overall, while these results cannot definitely show which molecules are adsorbed on Hz surface, they highlight the importance of studying the surface of Hz prior to its use in antimalarials evaluation or immune response tests since the chemical composition may be similar to the theoretical values despite the presence of adsorbed biomolecules. This was the case in this work for ewHz, where the survey XPS analysis was indistinguishable from that of HA.

Also, these results confirm the highly adhesive character of Hz, probably as a result of its amphiphilic nature [2], and prove that there are multiple biological compounds that can adhere to Hz, such as components of the digestive vacuole membrane, proteins, carbohydrates, lipids, and RBC membranes [2]. These compounds could be related to Hz formation and may also be implicated in the physiological effects observed during malaria infection [2]. Additionally, the residues derived from the purification procedure are likely to be part of the molecules adsorbed on Hz, and our elemental analysis clearly shows that the protocol used to purify Hz affects the composition and amount of species adsorbed on its surface.

To better understand the binding mechanism between biomolecules and Hz surface, we assessed the interaction between HA and some amino acids (see Supporting information Section S5.3). These molecules are not only the monomers of peptides and proteins [33], but they also represent traces of any of the enzymes used in the purification procedure [38], as well as the fragments left by the enzymes after proteolysis. We selected two basic amino acids, histidine (His) and arginine (Arg); two nonpolar, alanine (Ala) and leucine (Leu); and a polar one, serine (Ser), since all of them may interact with the amphiphilic Hz surface. All the selected amino acids present sp^3-N in their structure, and His and Arg also present sp^2-N; thus, their XPS N_{1s} spectra signals are similar to those of Hz samples and control experiments [34].

Fig. 5A shows the N_{1s} spectrum obtained from the surface of HA crystals after contact with amino acids. The spectrum shows three peaks located at 398.1, 399.4 and 401.4 eV, similarly to what we found on pwHz, ewHz (Fig. 3A and B, respectively), and on all our previous control experiments (Fig. 4A–C). This may indicate that amino acids and small peptides are the possible adsorbed biomolecules in the samples of washed Hz. Like in the previous control experiments, the 399.4 eV/398.1 eV peak area ratio (0.25 ± 0.14) is lower than that measured on pwHz and ewHz (Fig. 3D, blue and red, respectively). While this may be due to the concentration of amino acids used in this experiment (see Supporting information Section S5.3), this result shows that amino acids interact strongly with the surface of Hz and remain attached despite the washes with detergents and water.

Amino acids may be adsorbed onto HA and Hz via hydrophobic interactions (e.g. between the vinyl or methyl side chains of heme and the alkyl side chains of Ala and Leu [39]), or hydrogen bonding and electrostatic interactions (e.g. between the hydroxyl group of Ser or the amino group of Arg or His and the propionic acid chains of HA [40]).

3.3. Surface carboxylate groups act as main adsorption sites on Hz

To understand when hydrophobic interactions or hydrogen bonds and electrostatic interactions predominate, we masked the carboxylate groups on HA by esterification with 2,2,2-trifluoroethanol (TFE) (see Supporting information Section S4 and Fig. S4) [14], and we incubated the resulting fluorinated HA with the previously selected amino acids (see Supporting information Section S5.4). The difference in N_{1s} spectrum between this sample (Fig. 5B) and all other controls (Figs. 4 and 5A) is striking: the spectrum does not show a peak at 399.7 eV and overall, it is very similar to the N_{1s} spectrum measured on HA (Fig. 3C). This implies that amino acids did not adsorb significantly on fluorinated HA, and that the carboxylate groups on the surface of Hz are the crucial sites for biomolecule adsorption. The molecules on Hz may be either H-bonded or electrostatically interacting with carboxylates, as in our control experiments, or covalently bonded to them. In fact, amide bonds between amino groups and Hz carboxylate groups may be catalyzed in vivo by proteases [41] and ribosomes and non-ribosomal peptide synthetases, e.g. ATP-dependent enzymes and ATP-grasp enzymes [42]. Amide bonds are quite resistant to hydrolysis; thus, they could persist on Hz surface after thorough washes.

3.4. The cleaning procedure introduces partial contamination on Hz surface

Finally, we used MALDI-ToF to further analyze the molecules adsorbed on ewHz and pwHz. We compared the spectra relative to the fragments ablated from Hz crystals and from HA, and ascribed any signal present in the spectra of pwHz or ewHz but not in HA to molecules adsorbed on Hz. The HA spectrum (Fig. 6A, green) shows the characteristic MALDI fragment ion at *m/z* 616, which corresponds to an intact heme monomer [43]. In addition, other molecular masses related to the heme signature are observed at *m/z* 471, 484, 498, 511, 526, 557 and 571, as previously reported [43], The three peaks located in the low *m/z* region at 206, 224 and 246 (Fig. 6B, green) are assigned to ion fragments of sinapinic acid used as matrix (Fig. S5).

The mass spectrum of pwHz (Fig. 6A, blue) also shows the signal of intact heme; however, the peak intensity and peak resolution is lower compared to the HA spectrum. For example, some isotopic masses relative to the average masses of 498, 511 and 526 are lost; whereas the signals at *m/z* 471 and 484 associated with heme monomers are missing. This decrease in signal may be related to abundant species with high molecular weight adsorbed onto the surface of the crystals, which compete for the charges during the ionization process and suppress the signal from less abundant components [44]. These

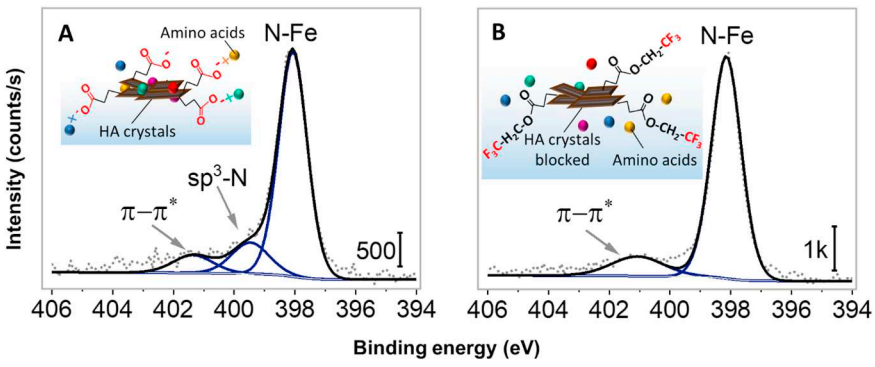

Fig. 5. XPS high resolution of the N_{1s} core level acquired for (A) HA after interacting with amino acids, (B) fluorinated HA crystals after interacting with amino acids. Experimental data are shown in dark gray dotted line, peak fits in blue and the overall fit in black. All data are representative of three independent experiments and three different spots analyzed along the same sample. (For interpretation of the references to color in this figure legend, the reader is referred to the web version of this article.)

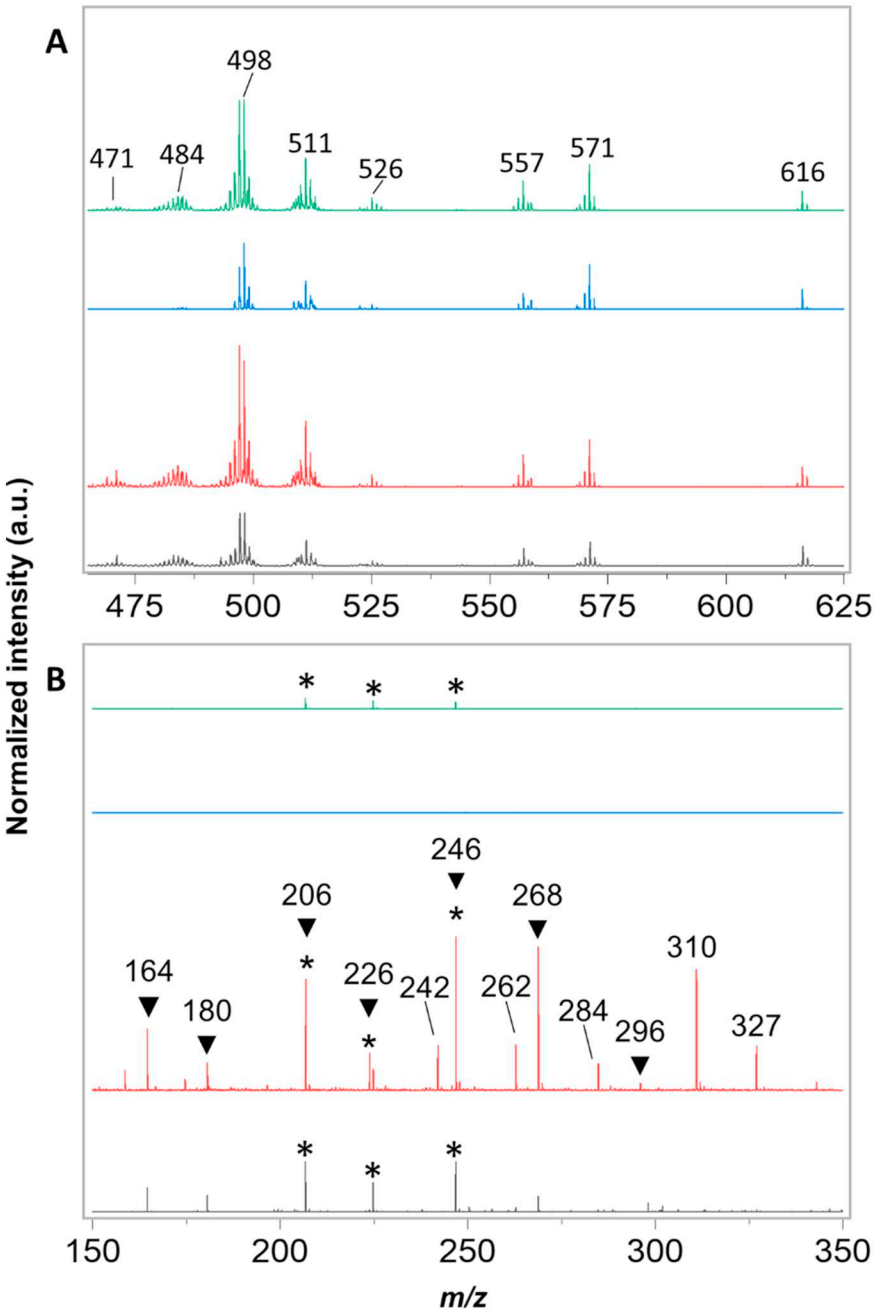

Fig. 6. Representative MALDI-ToF mass spectra of positive ions in reflectron mode collected in the *m/z* region of (A) 150–350 and (B) 465–625 for HA (green), pwHz (blue), ewHz (red) and HA treated with the extensive washes (black). All experiments were repeated three independent times with similar results. The intensity was normalized with respect to the intensity of the peak at 616 Da. The peaks related to the matrix are marked with an asterisk (*). The peaks arising after the washing procedure are marked with an inverted triangle (▼). (For interpretation of the references to color in this figure legend, the reader is referred to the web version of this article.)

macromolecules would require further preparation for mass spectra analysis; e.g. gel electrophoresis (SDS-PAGE or agarose) for proteins [44].

The mass spectrum of ewHz shows the heme signals in the *m/z* region of 471 to 616 (Fig. 6A, red). The spectral resolution and intensity are comparable to those found for HA (Fig. 6A, green), which confirms that the presence of large molecules on the surface of pwHz suppressed the MALDI signal of heme and related ions on that sample (Fig. 6A, blue), and this issue is solved by extending the purification procedure of Hz. However, several peaks appear in the low *m/z* region of the spectrum of ewHz (Fig. 6B, red), which are not present in the spectra of either HA (Fig. 6B, green) or pwHz (Fig. 6B, blue). We hypothesize that these signals are related to ion fragments of species produced by the enzymes used during the extensive purification, such as peptides and amino acids, as discussed before.

To prove this hypothesis, we collected the MALDI-ToF spectrum of HA treated with the extensive methodology used to obtain ewHz. The spectrum of this sample shows both the characteristic peaks of intact heme monomer in the *m/z* range of 471–616 (Fig. 6A, black), and peaks in the low *m/z* region (Fig. 6B, black). Some of these new peaks are in the same positions as the ion fragments present in the low *m/z* region of the ewHz spectrum (Fig. 6B, black, marked with an inverted triangle). Also, the peaks assigned to sinapinic acid at 206, 224 and 246 were significantly larger on both this sample and on ewHz than on HA, which suggests that some of the adsorbed biomolecules on ewHz and this sample produce ions with the similar molecular masses as the matrix.

4. Discussion

Understanding the surface properties of Hz has remained a major challenge due to the difficulty of isolating sufficient material from the parasites [45], and the lack of a standardized protocol to purify and characterize the crystals after extraction [14,16]. In this work, we used XPS and MALDI-ToF to compare the composition of Hz surface after

purification with an extensive methodology involving organic solvents, detergents and three types of enzymes, and a shorter one, which involves only one enzyme in the final treatment. In addition, we used synthetic HA crystals put in contact with biomolecules that mimic the natural environment of native Hz to understand the nature of the adsorbed molecules on Hz samples.

Our results showed that even after the extensive washing procedure several low molecular weight residues such as lipids, carbohydrates, amino acids and peptides persist on Hz surface, while after the shorter procedure larger amounts of contaminants of higher molecular weight are present. The molecules remaining after the shorter washing procedure also contained unexpected elements, such as calcium and silicon.

We did not detect any nucleic acids on either sample. This implies that the thorough purification activity in the extensive treatment cannot be attributed to the use of the DNase I and RNase A. Instead, the high pH of the buffers used to suspend the enzymes during the extensive wash may be responsible for the greater purification observed with this treatment since high pH degrades the outermost layer of Hz [2]. Thus, the addition of enzymes to degrade nucleic acids may not be necessary to treat Hz. Although the use of an alkaline buffer is essential to obtain cleaner crystals, there is a sacrifice in yield from this step.

The macromolecules found on both pwHz and ewHz may have adhered on Hz surface during its extraction from the parasite digestive vacuole and RBC; but they may also be fragments or whole proteins involved in the biocrystallization of Hz. Most biominerals are formed under the direction of proteins [46–48], which can then remain adsorbed at the biomineral surface or included within the crystals. Thus, even inorganic biominerals that show excellent crystallinity contain large amount of organic material [48]. In fact, Chugh *et al.* proposed that heme detoxification protein (HDP) rapidly converts heme into Hz [49], and Nakatani *et al.* suggested that some histidine residues in HDP direct the proper alignment of heme monomers to enable the formation of the axial ligand of the heme iron in Hz [50]. Thus, the biomolecules we found adsorbed onto Hz surface may be traces of its biomineralization process.

5. Conclusions and outlook

Our results show that the methodology chosen to purify Hz affects the surface of the crystals in terms of both amount and nature of contaminants. This explains the discrepancies related to the immunomodulatory properties of Hz. The use of different protocols to purify Hz produces crystals with different species on its surface that in turn modulate different host responses [2]. A standardized procedure that researchers could use prior to analyzing biological effects of Hz would clarify the state of Hz each work is dealing with, and prevent generating controversial results. We propose that XPS and MALDI-ToF become standard characterization tools to evaluate Hz surface since they require small amounts of sample and are highly sensitive.

The finding that carboxylate groups are critical for adsorption of molecules on Hz surface is of outstanding relevance for antimalarial drug design, particularly for those that act by inhibiting Hz growth [4]. Drug screening should probably focus on carboxylate binding candidates.

Overall, this work suggests that the surface of Hz may never be free from contaminants, and ultimately questions the concepts of “pure” Hz crystals. We showed that many compounds adhere onto the amphiphilic surface of Hz during its formation and extraction; but if these compounds adhere during the process of Hz crystallization, they are likely to be present not only at its surface, but also as integral components of the bulk of Hz crystals. Carboxylate groups, here shown to bind the adsorbed molecules, may serve as substrates for nucleation and growth inside the digestive vacuole of the parasite [51,52]. The organic coating bound to native Hz could be part of an organic matrix present within Hz structure to coordinate its crystal nucleation and formation [9,45]. The proposed mechanism raises an intriguing question: how much of the adsorbed molecules associated to Hz originates from contamination and how much represents material involved in the biomineralization? Further work is needed to explore this fascinating concept.

Abbreviations

HA	hematin anhydride
Hz	hemozoin
ewHz	extensively washed hemozoin
pwHz	partially washed hemozoin
sp^2-N	sp^2 hybridized nitrogen components
sp^3-N	sp^3 hybridized nitrogen components
RBC	red blood cell
MALDI-ToF	matrix-assisted laser desorption/ionization time of flight
XPS	x-ray photoelectron spectroscopy

Author contributions

The manuscript was written through contributions of all authors. All authors have given approval to the final version of the manuscript.

Notes

The authors declare no competing financial interest.

Acknowledgements

E. D. G. thanks Consejo Nacional de Ciencia y Tecnología (CONACyT) de México (CVU 354150), Secretaría de Educación Pública (SEP) de México (grant BC-3262), and the McGill Excellence Doctoral Award (MEDA). F. B. thanks King Abdulaziz University - Saudi Arabia, in coordination with the Saudi Cultural Bureau - Ottawa for their financial support. All the authors acknowledge the Canada Research Chairs (CRC) foundation and Natural Sciences and Engineering Research Council of Canada (NSERC) for funding.

Appendix A. Supplementary data

Electronic Supplementary Information (ESI) available: Details relative to materials and methods, XRD and FT-IR analysis of hematin anhydride, characterization of HA fluorinated with TFE, and details relative to the parameters used for XPS analysis of all samples. Supplementary data to this article can be found online at https://doi.org/10.1016/j.jinorgbio.2019.01.021.

References

[1] World Health Organization, World Malaria Report 2017, (2017).
[2] M. Boura, R. Frita, A. Góis, T. Carvalho, T. Hänscheid, The hemozoin conundrum: is malaria pigment immune-activating, inhibiting, or simply a bystander? Trends Parasitol. 29 (10) (2013) 469–476.
[3] S. Pagola, P.W. Stephens, D.S. Bohle, A.D. Kosar, S.K. Madsen, The structure of malaria pigment β-haematin, Nature 404 (6775) (2000) 307–310.
[4] K.N. Olafson, T.Q. Nguyen, J.D. Rimer, P.G. Vekilov, Antimalarials inhibit hematin crystallization by unique drug–surface site interactions, Proc. Natl. Acad. Sci. 29 (2017) 7531–7536 201700125.
[5] T.J. Egan, Recent advances in understanding the mechanism of hemozoin (malaria pigment) formation, J. Inorg. Biochem. 102 (5–6) (2008) 1288–1299.
[6] C.K. Carney, A.C. Schrimpe, K. Halfpenny, R.S. Harry, C.M. Miller, M. Broncel, S.L. Sewell, J.E. Schaff, R. Deol, M.D. Carter, The basis of the immunomodulatory activity of malaria pigment (hemozoin), JBIC, J. Biol. Inorg. Chem. 11 (7) (2006) 917–929.
[7] J.W. Griffith, T. Sun, M.T. McIntosh, R. Bucala, Pure hemozoin is inflammatory in vivo and activates the NALP3 inflammasome via release of uric acid, J. Immunol. 183 (8) (2009) 5208–5220.
[8] M. Olivier, K. Van Den Ham, M.T. Shio, F.A. Kassa, S. Fougeray, Malarial pigment hemozoin and the innate inflammatory response, Front. Immunol. 5 (2014) 25.
[9] M.T. Shio, F.A. Kassa, M.-J. Bellemare, M. Olivier, Innate inflammatory response to the malarial pigment hemozoin, Microbes Infect. 12 (12) (2010) 889–899.
[10] D. Taramelli, S. Recalcati, N. Basilico, P. Olliaro, G. Cairo, Macrophage preconditioning with synthetic malaria pigment reduces cytokine production via heme

iron-dependent oxidative stress, Lab. Investig. 80 (12) (2000) 1781.
[11] N. Thawani, M. Tam, M.-J. Bellemare, D.S. Bohle, M. Olivier, J.B. de Souza, M.M. Stevenson, Plasmodium products contribute to severe malarial anemia by inhibiting erythropoietin-induced proliferation of erythroid precursors, J. Infect. Dis. 209 (2013) 140–149 jit417.
[12] C. Casals-Pascual, O. Kai, J.O.P. Cheung, S. Williams, B. Lowe, M. Nyanoti, T.N. Williams, K. Maitland, M. Molyneux, C.R.J.C. Newton, N. Peshu, S.M. Watt, D.J. Roberts, Suppression of erythropoiesis in malarial anemia is associated with hemozoin in vitro and in vivo, Blood 108 (8) (2006) 2569–2577.
[13] O.A. Skorokhod, L. Caione, T. Marrocco, G. Migliardi, V. Barrera, P. Arese, W. Piacibello, E. Schwarzer, Inhibition of erythropoiesis in malaria anemia: role of hemozoin and hemozoin-generated 4-hydroxynonenal, Blood 20 (2010) 4328–4337.
[14] E.D. Guerra, D.S. Bohle, M. Cerruti, Surface characterization of hematin anhydride: a comparison between two different synthesis methods, Langmuir 32 (18) (2016) 4479–4484.
[15] J.N. Bulmer, F.N. Rasheed, N. Francis, L. Morrison, B.M. Greenwood, Placental malaria. I. Pathological classification, Histopathology 22 (3) (1993) 211–218.
[16] M. Jaramillo, M.-J. Bellemare, C. Martel, M.T. Shio, A.P. Contreras, M. Godbout, M. Roger, E. Gaudreault, J. Gosselin, D.S. Bohle, Synthetic plasmodium-like hemozoin activates the immune response: a morphology-function study, PLoS One 4 (9) (2009) e6957.
[17] E. Schwarzer, H. Kühn, E. Valente, P. Arese, Malaria-parasitized erythrocytes and hemozoin nonenzymatically generate large amounts of hydroxy fatty acids that inhibit monocyte functions, Blood 101 (2) (2003) 722–728.
[18] P. Parroche, F.N. Lauw, N. Goutagny, E. Latz, B.G. Monks, A. Visintin, K.A. Halmen, M. Lamphier, M. Olivier, D.C. Bartholomeu, R.T. Gazzinelli, D.T. Golenbock, Malaria hemozoin is immunologically inert but radically enhances innate responses by presenting malaria DNA to Toll-like receptor 9, Proc. Natl. Acad. Sci. 104 (6) (2007) 1919–1924.
[19] D. Wessel, U. Flügge, A method for the quantitative recovery of protein in dilute solution in the presence of detergents and lipids, Anal. Biochem. 138 (1) (1984) 141–143.
[20] C. Coban, K.J. Ishii, D.J. Sullivan, N. Kumar, Purified malaria pigment (hemozoin) enhances dendritic cell maturation and modulates the isotype of antibodies induced by a DNA vaccine, Infect. Immun. 70 (7) (2002) 3939–3943.
[21] M. Lvova, M. Zhukova, E. Kiseleva, O. Mayboroda, P. Hensbergen, E. Kizilova, A. Ogienko, V. Besprozvannykh, B. Sripa, A. Katokhin, Hemozoin is a product of heme detoxification in the gut of the most medically important species of the family Opisthorchiidae, Int. J. Parasitol. 46 (3) (2016) 147–156.
[22] G.S. Noland, N. Briones, D.J. Sullivan, The shape and size of hemozoin crystals distinguishes diverse Plasmodium species, Mol. Biochem. Parasitol. 130 (2) (2003) 91–99.
[23] B.R. Wood, E. Bailo, M.A. Khiavi, L. Tilley, S. Deed, T. Deckert-Gaudig, D. McNaughton, V. Deckert, Tip-enhanced Raman scattering (TERS) from hemozoin crystals within a sectioned erythrocyte, Nano Lett. 11 (5) (2011) 1868–1873.
[24] W. Trager, J.B. Jensen, Cultivation of erythrocytic and exoerythrocytic stages of plasmodia, in: J.P. Kreier (Ed.), Pathology, Vector Studies, and Culture, Academic Press, 1980, pp. 271–319.
[25] A. Klug, D. Rhodes, 'Zinc fingers': a novel protein motif for nucleic acid recognition, Trends Biochem. Sci. 12 (1987) 464–469.
[26] A.G. Shard, Detection limits in XPS for more than 6000 binary systems using Al and Mg Kα X-rays, Surf. Interface Anal. 46 (3) (2014) 175–185.
[27] R. Jugdaohsingh, Silicon and bone health, J. Nutr. Health Aging 11 (2) (2007) 99–110.
[28] F. Guntzer, C. Keller, J.-D. Meunier, Benefits of plant silicon for crops: a review, Agron. Sustain. Dev. 32 (1) (2012) 201–213.
[29] S.N.J. Moreno, L. Ayong, D.A. Pace, Calcium storage and function in apicomplexan parasites, Essays Biochem. 51 (2011) 97–110.
[30] J.L. Green, R.R. Rees-Channer, S.A. Howell, S.R. Martin, E. Knuepfer, H.M. Taylor, M. Grainger, A.A. Holder, The motor complex of Plasmodium falciparum phosphorylation by a calcium-dependent protein kinase, J. Biol. Chem. 283 (45) (2008) 30980–30989.
[31] S. Lourido, S.N.J. Moreno, The calcium signaling toolkit of the Apicomplexan parasites Toxoplasma gondii and Plasmodium spp, Cell Calcium 57 (3) (2015) 186–193.
[32] D.S. Bohle, A.D. Kosar, P.W. Stephens, The reversible hydration of the malaria pigment β-hematin, Can. J. Chem. 81 (11) (2003) 1285–1291.
[33] R.G. MacDonald, W.G. Chaney, Biochemistry, (2007).
[34] J.S. Stevens, A.C. Luca, M. Pelendritis, G. Terenghi, S. Downes, S.L. Schroeder, Quantitative analysis of complex amino acids and RGD peptides by X-ray photoelectron spectroscopy (XPS), Surf. Interface Anal. 45 (8) (2013) 1238–1246.
[35] P. Goldie, E.F. Roth, J. Oppenheim, J.P. Vanderberg, Biochemical characterization of Plasmodium falciparum hemozoin, Am. J. Trop. Med. Hyg. 43 (6) (1990) 584–596.
[36] B.L. Tekwani, L.A. Walker, Targeting the hemozoin synthesis pathway for new antimalarial drug discovery: technologies for in vitro beta-hematin formation assay, Comb. Chem. High Throughput Screen. 8 (1) (2005) 63–79.
[37] P. Kalantari, Rosane B. DeOliveira, J. Chan, Y. Corbett, V. Rathinam, A. Stutz, E. Latz, Ricardo T. Gazzinelli, Douglas T. Golenbock, Katherine A. Fitzgerald, Dual engagement of the NLRP3 and AIM2 inflammasomes by plasmodium-derived hemozoin and DNA during malaria, Cell Rep. 6 (1) (2014) 196–210.
[38] W. Ebeling, N. Hennrich, M. Klockow, H. Metz, H.D. Orth, H. Lang, Proteinase K from Tritirachium album limber, FEBS J. 47 (1) (1974) 91–97.
[39] J.S. Apte, G. Collier, R.A. Latour, L.J. Gamble, D.G. Castner, XPS and ToF-SIMS investigation of α-helical and β-strand peptide adsorption onto SAMs, Langmuir 26 (5) (2010) 3423–3432.
[40] T. Briggs, A.M. Chandler, Biochemistry, (1995).
[41] H.D. Jakubke, P. Kuhl, A. Könnecke, Basic principles of protease-catalyzed peptide bond formation, Angew. Chem. Int. Ed. Eng. 24 (2) (1985) 85–93.
[42] A. Goswami, S.G. Van Lanen, Enzymatic strategies and biocatalysts for amide bond formation: tricks of the trade outside of the ribosome, Mol. BioSyst. 11 (2) (2015) 338–353.
[43] P.A. Demirev, A.B. Feldman, D. Kongkasuriyachai, P. Scholl, D. Sullivan, N. Kumar, Detection of malaria parasites in blood by laser desorption mass spectrometry, Anal. Chem. 74 (14) (2002) 3262–3266.
[44] R. Matthiesen, Mass Spectrometry Data Analysis in Proteomics, 2nd ed., Humana Press, New York, 2013.
[45] T.J. Egan, Physico-chemical aspects of hemozoin (malaria pigment) structure and formation, J. Inorg. Biochem. 91 (1) (2002) 19–26.
[46] C.C. Perry, T. Keeling-Tucker, Biosilicification: the role of the organic matrix in structure control, JBIC, J. Biol. Inorg. Chem. 5 (5) (2000) 537–550.
[47] R.Z. LeGeros, Properties of osteoconductive biomaterials: calcium phosphates, Clin. Orthop. Relat. Res. 395 (2002) 81–98.
[48] L. Bergström, E.V. Sturm, G. Salazar-Alvarez, H. Cölfen, Mesocrystals in biominerals and colloidal arrays, Acc. Chem. Res. 48 (5) (2015) 1391–1402.
[49] D. Jani, R. Nagarkatti, W. Beatty, R. Angel, C. Slebodnick, J. Andersen, S. Kumar, D. Rathore, HDP-a novel heme detoxification protein from the malaria parasite, PLoS Pathog. 4 (4) (2008) e1000053.
[50] K. Nakatani, H. Ishikawa, S. Aono, Y. Mizutani, Identification of essential histidine residues involved in heme binding and Hemozoin formation in heme detoxification protein from Plasmodium falciparum, Sci. Rep. 4 (2014) 6137.
[51] X. Wang, E. Ingall, B. Lai, A.G. Stack, Self-assembled monolayers as templates for heme crystallization, Cryst. Growth Des. 10 (2) (2010) 798–805.
[52] S. Kapishnikov, T. Berthing, L. Hviid, M. Dierolf, A. Menzel, F. Pfeiffer, J. Als-Nielsen, L. Leiserowitz, Aligned hemozoin crystals in curved clusters in malarial red blood cells revealed by nanoprobe X-ray Fe fluorescence and diffraction, Proc. Natl. Acad. Sci. 109 (28) (2012) 11184–11187.